*ChemCatChem*

ChemCatChem
Chemistry Europe
European Chemical Societies Publishing

RESEARCH ARTICLE OPEN ACCESS

# Telomerization of Isoprene with Short Alcohols Using Novel Solid Molecular Phosphine Polymers

Julia Nikodemus[1] | Yaoyi Ren[1] | Isabella Kappel[2] | Felix Ott[1] | Claudia Weidenthaler[2] | Luke Keenan[3] | Peter J. C. Hausoul[1] | Regina Palkovits[1,4,5]

[1]Chair of Heterogeneous Catalysis and Technical Chemistry, Institut Für Technische aund Makromolekulare Chemie, RWTH Aachen University, Aachen, Germany | [2]Heterogeneous Catalysis, Powder Diffraction and Surface Spectroscopy, Max-Planck-Institut für Kohlenforschung, Mülheim an der Ruhr, Germany | [3]Diamond Light Source, Harwell Science and Innovation Campus, Didcot, UK | [4]Institute for a Sustainable Hydrogen Economy, Forschungszentrum Jülich GmbH, Jülich, Germany | [5]Max-Planck- Institute for Chemical Energy Conversion, Stiftstraße 34–36, Mülheim an der Ruhr, Germany

**Correspondence:** Peter J. C. Hausoul (hausoul@itmc.rwth-aachen.de) | Regina Palkovits (palkovits@itmc.rwth-aachen.de)

**Received:** 30 January 2026 | **Revised:** 16 March 2026 | **Accepted:** 2 April 2026

**Keywords:** heterogeneous catalysis | polyphosphines | solid molecular catalyst | telomerization | triphenylphosphine

## ABSTRACT

Palladium-loaded phosphine polymers have been designed and used as solid molecular catalysts (SMCs) in telomerization reactions with isoprene and short alcohols. A novel tris-(2-methoxyphenyl)phosphine-based polymer (pTOMPP), previously reported poly triphenylphosphine (pTPP) as well as TPP-based polymers with trigonal and tetragonal linkers were tested either pre-loaded or in-situ-loaded. The novel polymer pTOMPP proved to be an excellent support material during in-situ-loading, outperforming triphenylphosphine based polymers. Surprisingly pre-loaded SMCs resulted in significantly lower activity. XAS studies reveal that the enhanced activity of Pd/pTOMPP is due to the coordination sphere of Pd on the polymer showing a higher contribution of Pd-P bonds forming, whereas XAS spectra of Pd/pTPP show a higher contribution of inactive Pd-acac bonds. Especially pre-loaded polymers show little Pd-P interactions.

## 1 | Introduction

Telomerization reactions are C–C linking reactions of two 1,3-dienes with a nucleophile in the presence of palladium catalysts. They are usually run under neat conditions resulting in a broad range of possible products with 100% atom efficiency (Scheme 1). Over the last five decades, telomerization has been extensively studied in the field of homogeneous catalysis using various catalyst systems, dienes and nucleophiles [1]. Phosphine-based homogeneous catalysts have been reported to be active in the telomerization reaction for more than half a century. In 1967, Smutny [2] and Takahashi et al. [3]. performed the first telomerization reactions with Pd/triphenylphosphine (TPP) utilizing 1,3-butadiene as telogen and alcohols like phenol [2], as well as methanol, ethanol and isopropyl alcohol [3] or acetic acid [3], as nucleophiles. TPP was later also used for telomerization of butadiene with different nucleophiles such as $CO_2$ [4], CO/EtOH [5], and ammonia [6]. In 2008, Palkovits et al. compared different phosphine ligands in the telomerization of 1,3-butadiene with glycerol and reported that tris(2-methoxyphenyl)phosphine (TOMPP) outperforms TPP [7, 8]. The higher activity was attributed to positive effects of the electron donating and hemilabile coordinating methoxy groups. The substrate scope could be extended to various multifunctional nucleophiles having primary and secondary alcohol functions [9] as well as phenolic alcohols deriving from biomass [10–13]. Not only different nucleophiles, but various dienes have also been studied, in particular isoprene (Scheme 1). Isoprene is an asymmetric molecule resulting in 12 possible isomers as telomerization products. Linkage can occur in a tail-to-tail, head-to-head, tail-to-head or head-to-tail fashion, resulting in 8 possible *n*-isomers (including *E*- and *Z*-isomers), as well as 4 possible *iso*-isomers.

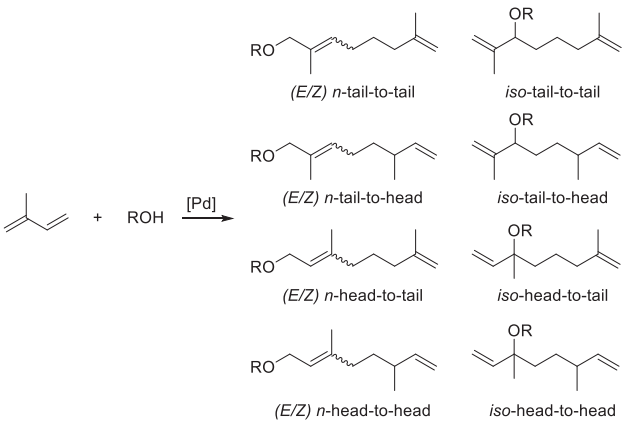


**SCHEME 1** | Telomerization of isoprene with an alcohol and the possible (*E/Z*)-*n*-telomers and *iso*-telomers.

The interest in isoprene telomerization stems from the structure of the reactant as it is the building unit for terpenes, such as citronellol or linalool, which are among the most important phytochemicals [16]. In addition, for the telomerization with isoprene, TPP was shown to be active with alcohols [17–20], especially methanol, and ammonia [21]. Recently, the focus of research has shifted from using phosphines to using N-heterocyclic carbenes (NHCs) as ligands because phosphine-based catalysts are significantly less regioselective than NHC based catalysts [22–25].

In recent years, considerable effort has been devoted to the development of solid molecular catalysts (SMCs) [26, 27] on the premise that SMCs can combine the advantages of homogeneous and heterogeneous catalysts. Ideally, incorporating single transition metal atoms in a solid host material retains the activity and selectivity of the corresponding homogeneous complex while at the same time allowing easy recycling of the catalyst [26, 28, 29]. Well-known representatives of such solid catalysts are metal organic frameworks (MOFs), which consist of metal clusters or ions with organic linkers, and covalent organic frameworks (COFs), in which the framework consists only of covalent bonds. Both systems are composed of rigid crystalline structures, that have a high surface area. However, studies have reported that the catalytic use of MOFs and COFs is limited by their chemical stability [30–32]. Therefore, porous organic polymers (POPs) have been introduced. Similar to MOFs and COFs, POPs are highly cross-linked macromolecules with rigid structures that provide high surface areas and controllable pore size distributions. They also tend to have high thermal and mechanical stability [33]. Catalytic activity is obtained by introducing metal ions or clusters via impregnation and immobilization by coordinative interactions [29, 32]. In this context, metal-loaded phosphine POPs can be an alternative system to industrially relevant molecular phosphine catalysts. Reports on heterogeneous catalysts for telomerization reactions are scarce. Most systems have been developed for the telomerization of butadiene with methanol. On the one hand, Pd was immobilized on silica and macroporous styrene/divinylbenzene resins [34]. Leaching of Pd into the solvent was found to be the main issue of the heterogenization. Only Pd/styrene/divinylbenzene anchored via 1,3-diphosphine ligands showed recyclability with a leaching of 1.6% in the first run. However, conversions were not found to exceed 20% with this reaction system [34]. Moreover, Pd/3,3',3''-phosphanetriyltris-(benzenesulfonic acid) trisodium (TPPTS) was immobilized on $KF/Al_2O_3$ [35] and double hydroxides [36], respectively. Both systems showed possible recyclability but low conversions. Wang et al. investigated the telomerization with a $Pd(OAc)_2$-loaded $PPh_3$-POP and obtained total isoprene conversion with the same efficiency as a homogeneous reference catalyst [37]. Recycling of the solid catalyst was possible for 11 consecutive runs without loss of isoprene conversion or regioselectivity. In addition, the reaction was successfully carried out on a large scale with a TON of 38812 to demonstrate the suitability of Pd-loaded POPs for industrial use. Furthermore, Zhang et al. presented a highly active heterogeneous catalyst based on a NHC-Polymer achieving a TON of 310624 after in-situ-loading with $Pd(OAc)_2$ [38]. Pre-loading led to a reduced TON of 8700 but the catalyst showed good recyclability without activity or selectivity loss after ten runs. For the telomerization with isoprene, only one heterogeneous approach has been reported by Torrente-Murciano et al. A catalyst system composed of Pd/1,1,3,3-tetramethyl-1,3-divinyldisiloxane complexes immobilized on a triphenylphosphine/divinylbenzene copolymer resin was used in the telomerization with methanol. The initial run showed a high conversion (85%) which decreased by 20% with every consecutive recycle run. The highest reported TON for this reaction system was 906 [39]. In 2013, Hausoul et al. reported the use of polyTPP, the polymeric analogue of TPP, in the telomerization reaction of butadiene with glycerol and phenol proving that the SMC outperformed its homogeneous counterpart [40]. Moreover, such metal-loaded poly phosphine polymers have been reported to be active in various reactions such as formic acid decomposition [41] and $CO_2$ hydrogenation [42, 43]. In this study, we present the use of four different ligands based on the triphenylphosphine motif: poly triphenylphosphine (pTPP), poly spiro-triphenylphosphine (pSTPP), poly tetraphenyl-methane-phosphine (pTPMP), and poly triphenyl-benzol-phosphine (pTPBP) (Scheme 2) in the telomerization reaction of isoprene with methanol and ethanol. In addition, we introduce a synthesis protocol for a novel polymer containing the TOMPP structure motive: poly tris(2-methoxyphenyl)phosphine (pTOMPP) and compare its activity to the triphenylphosphine based ligands.

## 2 | Results and Discussion

### 2.1 | Synthesis, Characterization, and Catalysis

All polymers were synthesized according to a previously developed protocol in which perlithiated arylbromides are cross-linked with $PCl_3$ and subsequently end-capped with PhLi (Scheme 2) [14, 15, 42]. The resulting polymers were characterized by solid state NMR (Figures S1–S10), $N_2$-physisorption (Table S1, Figures S14–S18), X-ray powder diffraction (XRD, Figure S19), thermogravimetric analysis (TGA, Figure S20), and scanning electron microscopy (SEM, Figures S21–22). TPP-based polymers show BET surface areas between 223 $m^2\ g^{-1}$ (pTPP) and 494 $m^2\ g^{-1}$ (pSTPP) and micropore volume areas between 43 $mm^3\ g^{-1}$ (pTPP) and 116 $mm^3\ g^{-1}$ (pTPBP). The lower surface area and micropore volume of pTPP in comparison to the other TPP-based polymers is expected as it is synthesized with the smallest linker and, as a result, possesses more compact pores. pTOMPP exhibits comparable physical properties as the TPP-based polymers. The

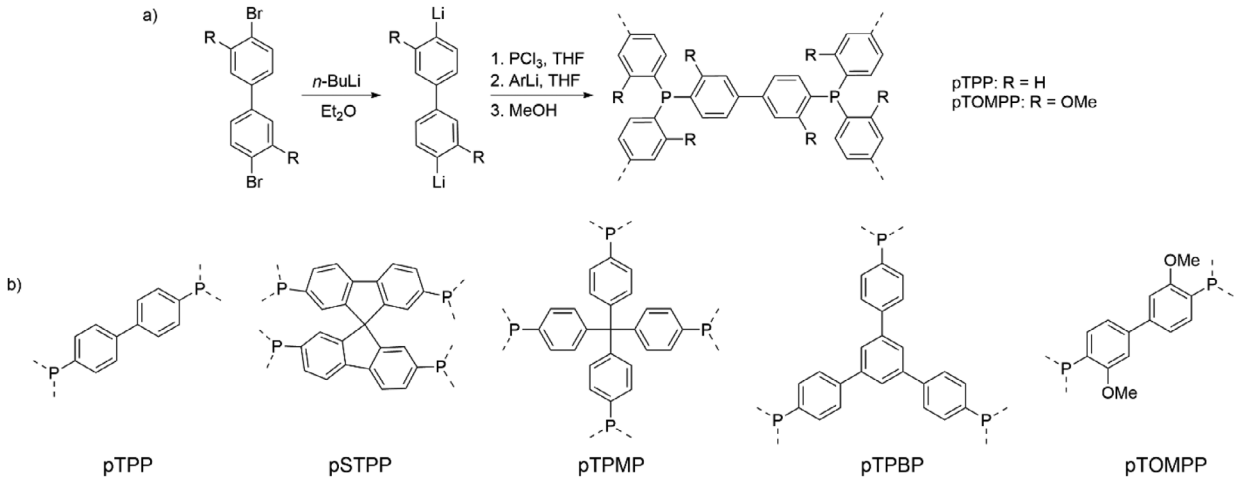


**SCHEME 2** | General synthesis of phosphine polymers [14, 15], exemplary shown for the formation of pTPP and pTOMPP (a) and synthesized phosphine polymers as ligands for the telomerization of isoprene with short alcohols in this study (b).

**TABLE 1** | Variation of P/Pd-ratio and Pd/$^{i}$Pr ratio on the telomerization of isoprene with MeOH for the ligands pTPP and pTOMPP.

| Entry | Polymer | *n* (Pd) [mmol] | P/Pd ratio | *n* ($^{i}$Pr) [mmol] | *Y*(telo) [%] | *X*($^{i}$Pr) [%] | Pd black formation |
|---|---|---|---|---|---|---|---|
| 1 | pTPP | 0.01 | 1.5 | 6.25 | 18 | 53 | yes |
| 2[a] | | 0.01 | 2.6 | 6.25 | 29 | 78 | yes |
| 3[a] | | 0.01 | 3.6 | 6.25 | 34 | 91 | — |
| 4 | | 0.01 | 4.6 | 6.25 | 34 | 87 | — |
| 5 | | 0.01 | 3.6 | 8.33 | 24 | 69 | yes |
| 6 | | 0.0075 | 3.6 | 6.25 | 19 | 59 | yes |
| 7 | | 0.005 | 5.2 | 4.50 | 18 | 63 | — |
| 8 | pTOMPP | 0.01 | 1.5 | 6.25 | 60 | 85 | yes |
| 9 | | 0.01 | 2.7 | 6.25 | 69 | 97 | — |
| 10 | | 0.01 | 3.6 | 6.25 | 45 | 67 | yes |
| 11 | | 0.01 | 4.6 | 6.25 | 65 | 97 | — |
| 12[a] | | 0.01 | 2.6 | 8.33 | 62 | 89 | yes |
| 13[a] | | 0.0075 | 2.6 | 6.25 | 73 | 88 | yes |
| 14 | | 0.005 | 5.2 | 4.50 | 52 | 80 | — |

Conditions: Methanol (2.28 mL), 80°C, 4 h, Nuc/Diene = 9

[a]Triple determination.

BET surface of pTOMPP is only 29 $m^2$ $g^{-1}$ and has no measurable micropore volume, confirming that the additional methoxy groups lead to an even denser polymer structure. In addition, TPP-based polymers are more thermally stable (decomposition starts at 370°C) than pTOMPP (decomposition starts at 260°C). All polymer materials show an X-ray-amorphous character and consist of particles with a broad particle size distribution according to SEM analysis.

Telomerization with methanol (MeOH) and ethanol (EtOH) were initially conducted under neat conditions using in-situ-loading (i.e. by adding metal precursor and pristine polymer separately together with isoprene ($^{i}$Pr) and the nucleophile). $Pd(acac)_2$ was chosen as metal precursor, as it leads to total isoprene conversion and it does not catalyze telomerization reactions without an additional ligand, thereby ensuring a heterogeneous catalytic reaction. The reaction has also been conducted with different Pd-precursors including $Pd(OAc)_2$, $Pd(PPh_3)_2(OAc)_2$, $PdCl_2$, and $Pd(dba)_2$ but all of those show little to no activity. Initially, a molar ratio of 9:1 of MeOH to $^{i}$Pr was applied as suggested by Berger et al. [18] for the telomerization of methanol using $Pd(acac)_2$ and TPP. $Pd(acac)_2$ was utilized with 0.16 mol% as previously reported for the telomerization of butadiene with glycerol using $Pd(acac)_2$/pTPP [15]. The activity of the catalyst depends on the applied P/Pd-ratio (Table 1). For pTPP, lower P/Pd ratios of 1.5 and 2.6 (Table 1, entries 1–4) lead to the formation of Pd black indicated by a color change of the polymer from yellow to brown. The nanoparticle aggregation on the SMC with a

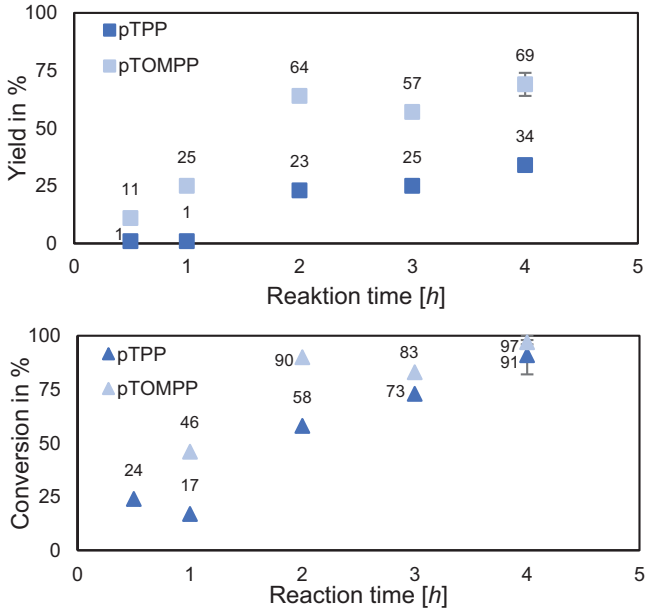


**FIGURE 1** | Time course of the telomerization of isoprene with methanol for the ligands pTPP and pTOMPP. Conditions: 80°C, Methanol (2.28 mL), 6.25 mmol isoprene, 0.01 mmol $Pd(acac)_2$, Nuc/Diene = 9, pTPP-Ligands: P/Pd = 3.6, pTOMPP: P/Pd = 2.7.

**TABLE 2** | Influence of the P/Pd ratio and the reaction time on the telomerization of isoprene with ethanol for the ligands pTPP and pTOMPP.

| Entry | Polymer | P/Pd | t [h] | *Y*(telo) [%] | *X*($^i$Pr) [%] | Pd black |
|---|---|---|---|---|---|---|
| 1 | pTPP | 2.6 | 5 | 0 | 19 | yes |
| 2 | | 3.6 | 2 | 0 | 20 | — |
| 3 | | 3.6 | 3 | 1 | 26 | — |
| 4 | | 3.6 | 4 | 2 | 39 | — |
| 5 | | 3.6 | 5 | 5 | 56 | — |
| 6 | | 3.6 | 6 | 6 | 68 | yes |
| 7 | pTOMPP | 2.6 | 2 | 23 | 55 | — |
| 8 | | 2.6 | 3 | 27 | 67 | — |
| 9 | | 2.6 | 4 | 43 | 89 | — |
| 10 | | 2.6 | 5 | 49 | 94 | — |
| 11 | | 2.6 | 6 | 47 | 96 | — |
| 12 | | 3.6 | 5 | 47 | 95 | — |

Conditions: Ethanol (3.28 mL), 80°C, 0.01 mmol Pd, 6.25 mmol. $^i$Pr, Nuc/Diene = 9.

P/Pd-ratio of 2.6 was confirmed by TEM-measurements (Figure S23). P/Pd ratios of 3.6 or 4.6 show no Pd black formation. Thus, the phosphine polymer appears to stabilize the metal precursor only at higher ratios without significant metal aggregation. This is also reflected in the telomer yields and isoprene conversions: the yield increases from 18% (P/Pd ratio of 1.5) to 29% (P/Pd ratio of 2.6) to 34% (P/Pd ratio of 3.6 and ratio of 4.6), while the conversion increases from 53% to 78% to 91% and 87%. Surprisingly, pTOMPP (Table 1, entries 8–11) shows nanoparticle aggregation at both low and higher P/Pd ratios of 1.5 and 3.6 by a change of the polymer color from orange to green or gray yielding 60% and 45% telomers, respectively. The aggregation of nanoparticles was confirmed by TEM measurements (Figure S24). The best yield (69%) and almost full conversion (97%) were achieved with a P/Pd ratio of 2.7 with no Pd black formation observed. As with pTPP, increasing the P/Pd ratio to 4.6 had no significant impact on the yield (65%) or conversion (97%).

It is worth noting that, under current conditions, the use of pTOMPP results in significantly higher yields than pTPP, suggesting that the methoxy groups play an important role in the telomerization reaction. Isoprene dimers are common side products for telomerization, which are also formed in this reaction. With pTOMPP less dimers are formed than with pTPP as ligands (Figure S25). The time course of the reaction was studied at P/Pd ratios of 3.6 (pTPP) and 2.7 (pTOMPP) using reactions that were stopped after 0.5, 1, 2, 3, and 4 h (Figure 1). After 2 h pTOMPP and pTPP resulted in 64% and 23% telomer yields, respectively. Subsequently the yields only increase slowly to 69% and 34% after 4 h. For pTPP, the conversion of isoprene increases from 17% to 58% and 73% to almost full conversion of 91% after 4 h for Pd@pTPP. For pTOMPP the isoprene conversion is faster with 46% after 1 h to full conversion of 97% after 4 h. The same trend but with less yields and conversion can be observed when using a P/Pd-ratio of 2,6 for pTPP and 3,6 for pTOMPP (Figure S26). Furthermore, the amount of Pd was reduced from 0.016 mol% to 0.012 mol% to minimize the necessary amount of Pd. First, the amount of Pd was kept at the initial 0.01 mmol but the $^i$Pr amount was increased (Table 1, entries. 5 and 12). This results in a decrease in activity from 34% to 24% telomer yield for pTPP and from 69% to 62% for pTOMPP. Second, the isoprene amount was kept at the initial 6.25 mmol and the Pd-amount was decreased (Table 1, entries 6 and 13) resulting in yields of 19% with pTPP and 73% with pTOMPP, respectively. In all four reactions, the isoprene conversions slightly decrease to 69% and 59% for pTPP and to 89% and 88% for pTOMPP. Against expectations, reducing the Pd-amount to 0.012 mol% by increasing the substrate amount or reducing the catalyst amount cause the formation of Pd black, which means that the catalyst is not stable under these reaction conditions. Finally, keeping 0.012 mol% Pd, the amount of precursor was reduced to 0.005 mmol while the P/Pd ratio was increased to 5.2 to maintain stability of Pd on the polymer (Table 1, entries 7 and 14). The reaction results in reduced activity with 18% and 52% telomer yields, as well as 63% and 80% isoprene conversions, but no Pd black formation. This indicates that a higher amount of Pd is necessary to catalyze the reaction and a higher P/Pd ratio is required to stabilize the Pd for this Pd/iPr ratio.

The telomerization of ethanol was carried out using the same P/Pd and Pd/$^i$Pr ratios as determined for methanol telomerization (Table 2). However, the polymers show a significant difference in activity for this reaction, as the polymer pTPP is almost not active at all (Table 2, entries 1–6). The highest telomer yield was determined to be 6% following a reaction time of 6 h, with an isoprene conversion of 68%. Isoprene dimers are the main product of this reaction. pTOMPP as ligand exhibits activity in ethanol telomerization, facilitating telomer yields up to 49% after 5 h with an almost full isoprene conversion of 94% (Table 2,

**TABLE 3** | Telomer yield and isoprene conversion after the telomerization of isoprene with either methanol or ethanol via in-situ-loading with $Pd(acac)_2$ and the corresponding ligand (Scheme 1).

| Polymer | *Y* (telo) [%] MeOH | *X* ($^i$Pr) [%] MeOH | *Y* (telo) [%] EtOH | *X* ($^i$Pr) [%] EtOH |
|---|---|---|---|---|
| pTPP | 34 | 91 | 2 | 34 |
| pSTPP | 33 | 97 | 7 | 85 |
| pTPMP | 39 | 93 | 1 | 26 |
| pTPBP | 44 | 97 | 7 | 64 |
| pTOMPP | 69 | 97 | 43 | 88 |

Conditions: 80°C, 4 h, Methanol (2.28 mL), 5 h, Ethanol (3.28 mL), 6.25 mmol isoprene, 0.01 mmol $Pd(acac)_2$, Nuc/Diene = 9, pTPP-Ligands: P/Pd = 3.6, pTOMPP: P/Pd = 2.7. Triple determination.

entries 7–12). In contrast to the reaction with methanol, a P/Pd ratio of 3.6 does not result in Pd black but in the same activity as a ratio of 2.7. Overall, the same trend as for MeOH can be seen. Using pTOMPP as a ligand results in better activity than pTPP. Furthermore, the use of MeOH as nucleophile has been demonstrated to yield significantly higher activity in comparison to the utilization of EtOH as nucleophile. The difference in reactivity between methanol and ethanol can be attributed to the greater nucleophilicity and reduced steric hindrance of methanol compared to ethanol.

In addition, acidity also plays a significant role. Ethanol has a slightly higher pKa value than methanol, meaning it is less likely to be protonated [44]. Deprotonation of the nucleophile is an essential step in the telomerization cycle before the nucleophilic attack [1]. The more basic the phosphine, the more electron-rich and basic the intermediate complex, and the more easily it can deprotonate the nucleophile. The methoxy groups in the ortho position relative to the phosphine in pTOMPP provide electron density to the phosphine, making it more electron-rich. Consequently, complexes with pTOMPP as ligand can deprotonate ethanol and catalyze the reaction, whereas the less basic and electron-poorer pTPP cannot.

The novel polymers pSTPP, pTPMP, and pTBP were screened under the best conditions found for pTPP and compared to pTOMPP (Table 3). The catalytic results show, that the in-situ-loaded triphenylphosphine based polymers perform similarly with telomer yields between 33% and 44% and almost full conversions. However, when tested with ethanol, all the catalysts show significantly lower telomer yields between 1% and 7% and conversions as observed before for pTPP. Various scientific studies suggest adding bases to facilitate deprotonation of the nucleophile and thereby improving the reaction efficiency [8, 37, 45]. Against expectations, adding NaOMe to the telomerization of isoprene with methanol or ethanol does not influence the reaction at all as the same yields are obtained. In fact, a change in the color of the polymer to green/grey indicating nanoparticle aggregation is observed. The novel heterogeneous ligand pTOMPP shows a telomer yield of 69% for methanol telomerization and a telomer yield of 43% for ethanol telomerization. It not only outperforms the triphenylphosphine-based polymers in the reaction with methanol, but also shows a remarkable activity in the reaction with ethanol. This indicates that the specific surface does not correlate with the catalytic activity in this case. Evidently, the methoxy group plays an important role in the coordination process of the dienes to the metal center facilitating the reaction. This is consistent with previous literature, which has demonstrated that electron-donating and hemi-labile coordinating methoxy groups have a positive influence on activity [7, 8]. Overall, the catalytic system Pd/pTOMPP exhibits significant activity in the telomerization with both nucleophiles indicating the robust capability and considerable potential of pTOMPP to stabilize the catalytic system.

**TABLE 4** | Recycling experiment for Pd/pTOMPP by starting off with the usual in-situ-reaction and subsequent filtration of the catalyst under Ar atmosphere. New solvent and substrate were added with every run.

| Recycling run | *Y* (telo) [%] | *X* ($^i$Pr) [%] | Color of the catalyst |
|---|---|---|---|
| 1 | 53 | 88 | Yellow |
| 2 | 7 | 66 | yellow/light green |
| 3 | 1 | 36 | green |
| 4 | 0 | 35 | dark green |
| 5 | 0 | 32 | dark green/grey |

Conditions: 50 mL glass pressure flask, 80°C, 4 h, 31.25 mmol isoprene, Nuc/Diene = 9, in-situ-loading: 0.05 mmol $Pd(acac)_2$, P/Pd = 2.7.

## 2.2 | Recycling Experiment

Recycling experiments were conducted with the in-situ-loaded pTOMPP catalyst in a 50 mL pressure flask instead of 10 mL pressure tube as used before. After every run the catalyst was filtered under Ar atmosphere and new solvent and substrate were added to the reaction system (Table 4). The first run results in a telomer yield of 53%. Subsequently, the activity decreases significantly and only 7% yield is obtained in the second run. From the fourth run on no activity is observed. The conversion also decreases with each run, indicating that the loss of activity is not due to decreasing selectivity but due to catalyst deactivation.

It is proposed that the resting state of Pd in the catalytic cycle is a Pd° complex [46–49]. Pd° complexes are prone to aggregation which results in Pd-nanoparticles. As the reaction requires a high metal content, such aggregation is highly likely. TEM

**TABLE 5** | Telomer yields and isoprene conversion after the telomerization of isoprene with methanol and the corresponding pre- or in-situ-loaded polymer.

| | *wt%* Pd | P/Pd | *Y*(telo) [%] | *X*($^i$Pr) [%] | TON |
|---|---|---|---|---|---|
| Pd@pTPPPre-loaded | 5.8 | 6.7 | 0 | 16 | 0 |
| Pd@pTPPIn-situ-loaded | 7.8 | 4.8 | 34 | 91 | 140 |
| Pd@pTOMPPPre-loaded | 4.7 | 6.2 | 32 | 50 | 185 |
| Pd@pTOMPPIn-situ-loaded | 6.1 | 4.7 | 69 | 97 | 404 |

Conditions: 80°C, 4 h, 6 25 mmol isoprene, Nuc/Diene = 9, in-situ-loading: 0.01 mmol $Pd(acac)_2$, L/M = 3.6 (pTPP), L/M = 2.7 (pTOMPP), pre-loaded: *m*(pre-loaded polymer) = 9.3 mg.

studies have shown that the spent in-situ-loaded catalyst already has Pd-nanoparticles on its surface after one run (Figure 4). In subsequent runs, these nanoparticles can agglomerate, as indicated by the color of catalyst as with higher nanoparticle formation and aggregation, the color of the catalyst darkens in each recycling run.

## 2.3 | Preloading of pTPP and pTOMPP

pTPP and pTOMPP were pre-loaded with the metal precursor $Pd(acac)_2$ in a wet-impregnation approach and then applied in the telomerization reaction with methanol (Table 5).

Against expectations, the pre-loaded catalysts show significantly reduced activity compared to the in-situ-loaded systems. Pre-loaded Pd@pTPP shows no activity whereas in-situ-loading results in 34% yield. Also, for Pd@pTOMPP in-situ-loading increases the yield from 32% to 69%. The metal amount was chosen such that a similar loading is obtained as for the in-situ-loaded case. However, ICP revealed a lower loading of the pre-loaded polymers with 5.8wt% instead of 7.8wt% for Pd@pTPP and 4.7wt% instead of 6.1wt% for Pd@pTOMPP (Table 5). In general, a P/Pd ratio of 6.7–6.2 for the pre-loaded, and a P/Pd ratio of 4.8 – 4.7 for in-situ-loaded species are determined for pTPP and pTOMPP, respectively. This indicates, that either during the in-situ-loading more P-sites are accessible for Pd-loading or the coordination sphere differs for pre-loading and in-situ-loading. Moreover, the higher loading of pTPP could be explained based on its higher specific BET-surface. To understand why the differently loaded catalysts show different activities, various characterization techniques were applied, including solid state NMR, XPS, TEM, and XAS of the pristine catalysts and the in-situ-loaded ones. First, solid-state $^{31}$P-NMR measurements were performed to determine if interactions of the phosphines of the polymer can be observed by chemical shifts. Initially, the spectra of pTPP with Pd loadings of 0.1%, 1%, and 5.8% were compared (Figure 2). The intensity of the initial P signal at −4 ppm decreases with the increase of Pd content in the polymer while a new signal appears at 31.5 ppm. The intensity of this new species increases with increased Pd content, due to interaction with Pd. Unexpectedly, for the 5.8 wt% Pd-loaded polymer (P/Pd = 6.7) the signal of the initial phosphorous has disappeared. The same can be observed in the spectra of the 7.7 wt% in-situ-loaded polymer (P/Pd = 4.8). One possible reason for this is the oxidation of the remaining phosphorus species, as the in-situ-polymer was filtered under air.

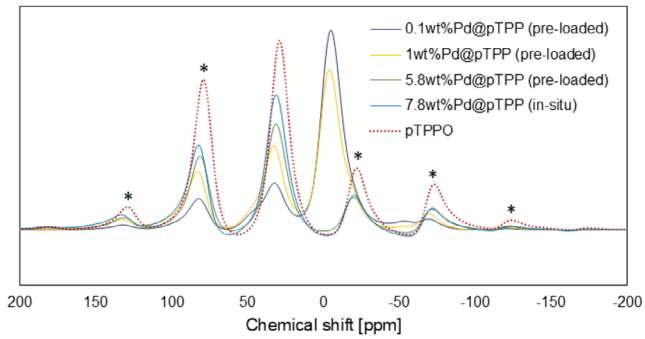


**FIGURE 2** | Solid state $^{31}$P-NMR of 0.1wt%,1wt%, and 5.8wt% Pd pre-loaded pTPP and 7.8wt%Pd in-situ-loaded polymer, as well as oxidized pTPP. Spinning side bands are marked with a star (*).

The pure pTPP polymer was oxidized to pTPPO, which gave a signal at 29 ppm. As the signal maxima of the 5.8 wt% pre-loaded polymer and the 7.8wt% in-situ-loaded polymer are between 31.5 ppm (P-Pd interaction) and 29 ppm (oxidized P), it is likely that the signal represents a mixture of both species. The same can be observed for Pd loaded on pTOMPP (Figure S11).

The normalized P2p XPS high resolution spectra of the in-situ- and pre-loaded catalysts as well as pristine polymers are shown in Figure 3. The pure polymers show peaks at 130 eV and 133 eV, corresponding to the tertiary phosphine and phosphine oxide respectively. The phosphine oxide can be attributed to oxidation as the XPS samples were prepared under air. For both pTPP and pTOMPP, the peak completely shifts to 132 eV due to loading with $Pd(acac)_2$. The Pd3d XPS high resolution spectra confirms that the major fraction of Pd species on the surface of the polymers is in the range of $Pd^{2+}$ with 337.7 eV. A small amount of $Pd^0$ is observed at 335.7 eV.

TEM measurements show the presence of Pd-nanoparticles on the surface of all catalysts (Figure 4). Interestingly, in the case of Pd@pTOMPP the surface is mostly clean with only a few isolated particles, indicating increased stability of the Pd-complexes. This raises the question whether nanoparticles have an effect on the reaction. Therefore, Pd-nanoparticles (Pd-NP) with an average particle size of 5–6 nm were synthesized and loaded onto the polymers. TEM (Figure 4) confirms that the size of the nanoparticles is on average the same as those of the original catalyst. Solid state $^{31}$P-NMR (Figures S12 and S13) indicates that no coordination takes place at the phosphine site, which is consistent with the catalytic results as no catalytic activity was

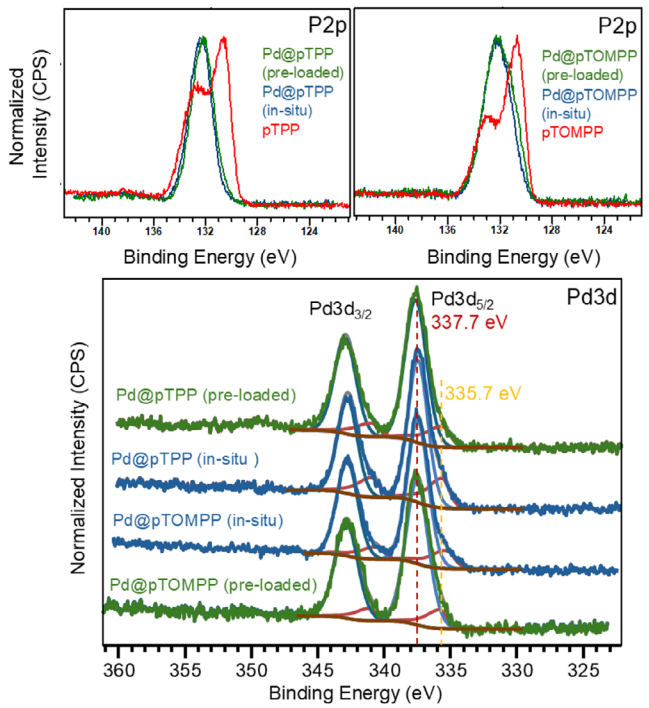


**FIGURE 3** | Normalized P2p XPS high resolution spectra of pTPP and pTOMPP in-situ- and pre-loaded in comparison to the unloaded pure polymers, as well as Pd3d XPS spectra of the catalyst species Pd@pTPP and Pd@pTOMPP in-situ- and pre-loaded.

observed during the telomerization reaction with Pd-NP loaded polymers.

## 2.4 | XAS Analysis of the Immobilized Species

As none of the previously demonstrated analytical methods provided insight into the origin of the catalysts' different activities, XAS measurements were performed (Figure 5). Previous studies have shown that XANES and EXAFS measurements can provide valuable insights into the chemical coordination of SMCs [50–52]. XANES spectra (Figure 5a) reveal information about the structure of catalysts by providing details of their oxidation state and ligands atoms. The edge energy E0 was determined using the first maximum of the derivative (Figure 5b). $Pd^0$, as present in the Pd-foil has an adsorption energy of 24350 eV, whereas $Pd^{2+}$, as present in the metal precursor $Pd(acac)_2$ has an adsorption energy of 24354 eV. The XANES spectra reveal an absorption edge energy for the pre-loaded Pd/pTPP catalyst within the expected range for the $Pd^{2+}$ oxidation state (24354 eV). The in-situ-loaded Pd/pTPP catalyst (24352 eV), as well as both Pd/pTOMPP (pre-loaded: 24352 eV and in-situ-loaded: 24351 eV) species range in between the absorption energies of $Pd^0$ and $Pd^{2+}$. This could be due to the presence of various Pd species in the catalyst samples.

Figure 5c compares the EXAFS spectra of the Pd@pTPP catalyst species in comparison to Pd-foil as Pd-Pd bond reference, $Pd(acac)_2$ as Pd–O bond reference of the precursor and $Pd[PPh_3]_4$, as well as $Pd(acac)_2$+TPP, for Pd-P bond reference. The sample denoted "$Pd(acac)_2$+TPP" was prepared by stirring $Pd(acac)_2$ with TPP (P/Pd ratio of 3.6) in methanol at 80°C for 4 h. A

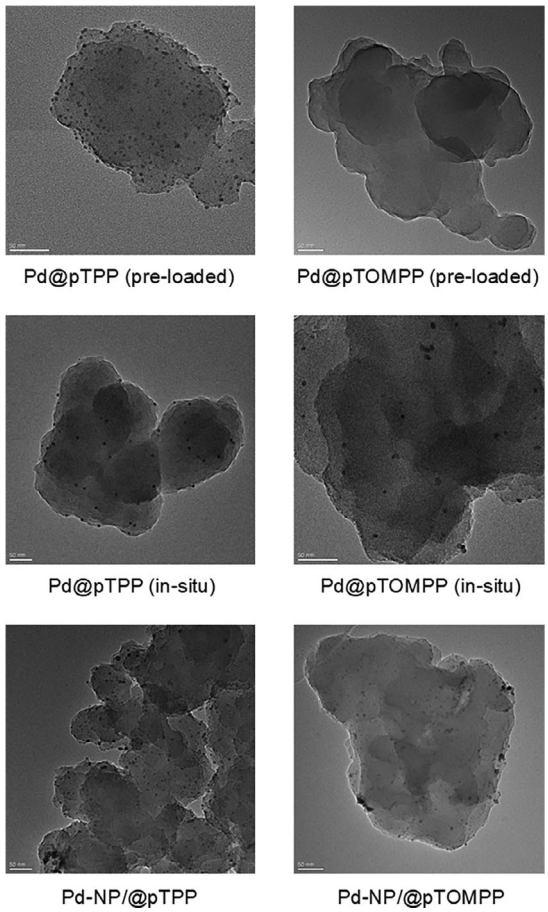


**FIGURE 4** | TEM images (50x) of the catalyst species Pd@pTPP and Pd@pTOMPP in-situ- and pre-loaded, as well as pTPP and pTOMPP loaded with Pd-NP.

solid precipitated which was filtered and dried. Liquid $^1H$ and $^{13}C$ NMR spectra revealed the absence of acac signals. In $^{31}P$ NMR a signal at 25.5 ppm was observed. This is in accordance with the $^{31}P$ spectrum of commercially available $Pd[PPh_3]_4$. Furthermore, the EXAFS spectrum of $Pd(acac)_2$+TPP was compared with that of the metal precursor $Pd[PPh_3]_4$, which proved nearly identical. This confirms that the acac ligands were exchanged by phosphines. The spectra reveal that there is no significant overlap between the catalyst samples and the reference spectra for Pd–Pd, Pd–O, and Pd–P bonds. This suggests that the catalyst samples consist of a mixture of different Pd interactions. No Pd–Pd bonds can be observed at all in the catalysts, verifying that the majority of the Pd-complexes are molecularly dispersed. The maximum of the EXAFS peaks of the Pd@pTPP catalysts are in between the signals for Pd–O and Pd–P bonds suggesting a contribution of both interactions. The pre-loaded catalyst is shifted more towards the Pd–O peak, whereas the in-situ-loaded catalyst is shifted more towards the Pd–P peak. This suggests that the in-situ-loaded catalysts has a higher contribution of Pd–P interactions than to the pre-loaded catalyst.

Figure 5d shows the EXAFS spectra of the Pd@pTOMPP catalysts in comparison to Pd-foil as Pd–Pd bond reference, $Pd(acac)_2$ as Pd–O bond reference of the precursor and $Pd(acac)_2$+TOMPP, for Pd–P bond reference. $^1H$ and $^{13}C$ NMR spectra of $Pd(acac)_2$+TOMPP also show no acac signals

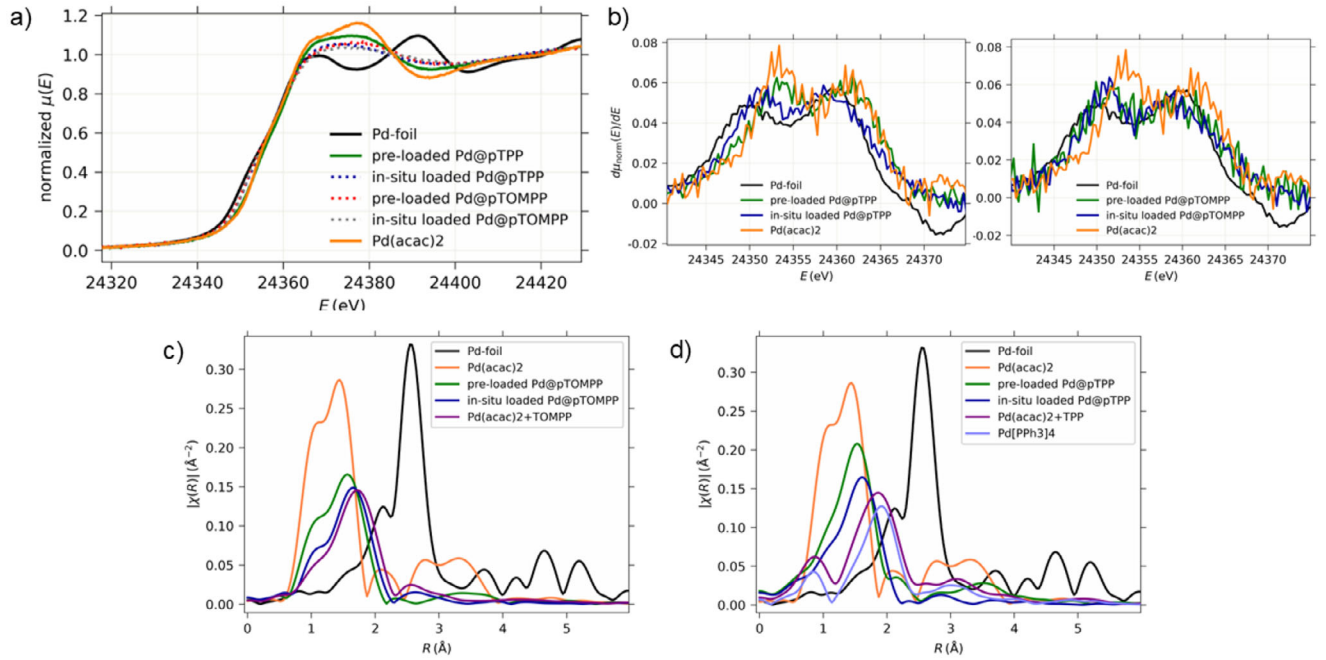


**FIGURE 5** | XANES spectra of Pd loaded polymers pTPP and pTOMPP in comparison to $Pd^0$ (Pd-foil) and $Pd^{2+}$ ($Pd(acac)_2$) (a) and the first derivative of the spectra (b), as well as EXAFS spectra of references and Pd-loaded pTPP (c) and pTOMPP (d) catalysts, as well as the metal precursor $Pd(acac)_2$.

and a $^{31}P$ signal at 21.79 ppm. The EXAFS spectra of the pre-loaded Pd@pTOMPP catalyst shows the maximum shifted more towards the Pd-P bond length but generally falling between the Pd-O and Pd-P signals. In contrast, the EXAFS spectrum of the in-situ-loaded Pd@pTOMPP overlaps significantly with the EXAFS spectrum of the $Pd(acac)_2$+TOMPP, indicating that the Pd-P contribution is dominant in this catalyst. This structural similarity to the molecular Pd-P species may be the reason for the advanced activity of these catalysts.

XANES and EXAFS show that the in-situ-loaded catalysts exhibit a higher P–Pd contribution, which appears to be the reason for their increased activity. In order to understand the loading process, a closer look at the catalytic cycle is required. The catalytic cycle was proposed by Jolly et al. for the telomerization of butadiene with methanol [46–49]. Therein a $[Pd^0(PPh_3)(\eta^2\text{-diene})_2]^0$ complex is considered to be the active complex, in which the C–C coupling occurs resulting in a $[Pd^{II}(PPh_3)(\eta^3,\eta^1\text{-octadiendiyl})]^0$ complex. This complex is then protonated by the nucleophile (ROH) to yield $[Pd^{II}(PPh_3)(\eta^3,\eta^2\text{-octadienyl})]^+$ $RO^-$. Following the nucleophilic attack, the product complex $[Pd^0(PPh_3)(\eta^2,\eta^2\text{-1-RO-octadiene})]$ is obtained which after ligand exchange with dienes releases the product and completes the cycle. In 2025, Bouley et al. published a study where the mechanism of the formation of the active catalyst from $Pd(acac)_2$ and TPP in the telomerization of methanol with butadiene was investigated [53]. As already published by Kanda et al. [54]. and Suslov et al. [55]., the combination of $Pd(acac)_2$ and TPP results in the formation of a $[Pd^{II}(acac)_2(PPh_3)]$ complex where one acac ligand changes from $\kappa^2$-O,O to the $\kappa^1$-C binding mode. In addition to that, the complex $[Pd^{II}(acac)(PPh_3)_2]^+$ can form. It is postulated that this complex undergoes a reductive elimination of one acac and one $PPh_3$ ligand to yield a $[Pd^0(PPh_3)]$ complex that can enter the cycle via the coordination of two diene ligands (Scheme 3) [53]. However, the $[Pd^{II}(acac)_2(PPh_3)]$ complex is quite stable

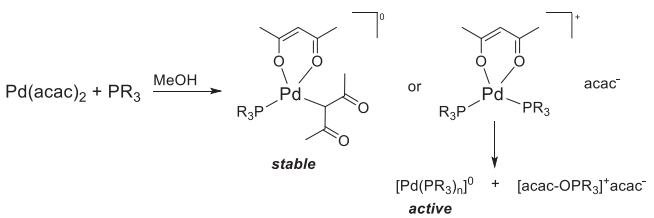


**SCHEME 3** | Formation of the stable $[Pd^{II}(acac)_2(PR_3)]^0$ or the $[Pd^{II}(acac)(PR_3)_2]^+$.complex which results the active $[Pd(PR_3)_n]^0$ catalyst [53].

and it was demonstrated that it can be transformed to the active $[Pd^{II}(acac)(PPh_3)_2]^+$ complex via addition of acids, like AcOH [54] or $BF_3$ [55].

The EXAFS results clearly show that the pre-loading of $Pd(acac)_2$ on the polymer pTPP resulted in the formation of the stable $[Pd^{II}(acac)_2(pTPP)]$ complex as one of the main species. This is supported by XPS which identifies $Pd^{2+}$ as dominant species and XANES which shows a similar absorption edge as $Pd(acac)_2$. Therefore, the high specific surface area measured by BET is not an advantage in this case, as it is occupied by inactive species. Pre-loaded Pd@pTOMPP also shows $Pd^{2+}$ as the main Pd-species. In this polymer, the methoxy group acts both as a directing ligand and hemilabile ligand. The coordination of the methoxy group to Pd may facilitate ligand exchange which can aid in the loss of one acac ligand, enabling the formation of the active $[Pd^{II}(acac)(PPh_3)_2]^+$. Therefore, the catalyst has a high catalytic activity even though it exhibits a low specific surface area. The presence of the dienes during catalyst formation appears to have a positive impact for both polymers. Furthermore, the presence of a hemilabile ligand in the support material influences the formation of the complex, improving it during in-situ-loading.

## 3 | Conclusion

Five phosphine polymers, four based on the TPP motif and one based on the tris(2-methoxy-phenyl)phosphine (TOMPP) motif, were designed and applied as ligands in the telomerization reaction of isoprene with the short alcohols methanol and ethanol. The introduced TOMPP-based polymer (pTOMPP), in-situ-loaded with Pd, showed enhanced activity during telomerization with methanol (68% telomer yield) and ethanol (43% telomer yield) compared to the TPP-based polymers with 32%–43% and 1%–7% telomer yields, respectively. In addition, the in-situ-loaded species of Pd@pTPP and Pd@pTOMPP showed enhanced activity in methanol compared to their corresponding pre-loaded catalyst species with only 0% and 31% telomer yields, respectively. XPS measurements display the same oxidation state of $Pd^{2+}$ and solid state $^{31}$P-NMR analysis shows similar chemical shifts. This indicates that the changed reactivity could be evident of different coordination modi which could not be characterized so far. Recent XAS studies, particularly EXAFS and XANES studies have confirmed that the coordination sphere around the Pd center varies depending on the loading process and the support materials used. Following pre-loading, the catalysts exhibit contributions from Pd–O and Pd–P bonds, indicating that acac ligands from the precursor are retained. Pre-loading on pTPP in particular results in an inactive, stable $[Pd^{II}(acac)_2(PR_3)]^0$ complex. The support material pTOMPP, which has a methoxy group as a hemilabile ligand has a positive influence on the pre-loading process, enabling the formation of an active catalyst species during catalysis. In-situ-loading provides better conditions for enhanced P–Pd character, as the presence of dienes helps to form the active species. Support materials with a directing ligand also have a positive influence on the loading process, as shown by EXAFS of Pd@pTOMPP, which revealed mainly Pd-P bond contributions. These findings of metal coordination on different support materials under different loading conditions mark an important step in the analysis of the coordination-activity relationship of SMCs, as these could not be identified from the previous broad range of analyses. This will help to improve the loading process for solid molecular catalysts in the future.

### Author Contributions

**Isabella Kappel:** writing – review and editing, data curation, formal analysis. **Claudia Weidenthaler:** writing – review and editing, supervision, methodology. **Julia Nikodemus:** writing – original draft, investigation, formal analysis, data curation, conceptualization. **Peter J. C. Hausoul:** supervision, writing – review and editing, conceptualization. **Yaoyi Ren:** investigation, data curation. **Regina Palkovits:** writing – review and editing, supervision, resources, project administration, methodology, funding acquisition, conceptualization. **Felix Ott:** writing – review and editing, investigation, data curation. **Luke Keenan:** writing – review and editing, formal analysis, methodology, validation.

### Acknowledgments

We kindly thank C. Franzen, H. Eschmann, and H. Fickers-Boltz for GC, as well as GC-MS measurements and N. Avraham-Radermacher for BET, XRD and TG measurements. In addition, we thank F. Müller (TEM, XAS) and J. Baums (XAS) for taking part in the analytic measurements. We kindly thank Frederic Thilmany for conducting catalysis experiments. We acknowledge funding by the Cluster of Excellence Fuel Science Center (EXC 2186, ID: 390919832) by the Excellence Initiative by the German federal and state governments to promote science and research at German universities as well as the RWTH Prep Fund Project EXC2186,"The Fuel Science Center,". We further thank the Diamond Light Source for providing beamtime on the beamline B18 (Experiment No. SP36175-1).

### Conflicts of Interest

The authors declare no conflicts of interest.

### Data Availability Statement

The data that supports the findings of this study are available in the supplementary material of this article.

### References

1. A. Behr, M. Becker, T. Beckmann, L. Johnen, J. Leschinski, and S. Reyer, "Telomerisation—Fortschritte und Anwendungen einer Vielseitigen Reaktion," *Angewandte Chemie* 121 (2009): 3652–3669, https://doi.org/10.1002/ange.200804599.

2. E. J. Smutny, "Oligomerization and Dimerization of Butadiene Under Homogeneous Catalysis. Reaction With Nucleophiles and the Synthesis of 1,3,7-octatriene," *Journal of the American Chemical Society* 89 (1967): 6793–6794, https://doi.org/10.1021/ja01001a089.

3. S. Takahashi, T. Shibano, and N. Hagihara, "The Dimerization of Butadiene by Palladium Complex Catalysts," *Tetrahedron Letters* 8 (1967): 2451–2453, https://doi.org/10.1016/S0040-4039(00)90830-X.

4. A. Behr, P. Bahke, and M. Becker, "Palladium-katalysierte Telomerisation von Kohlendioxid mit Butadien im Labor- und Miniplantmaßstab," *Chemie Ingenieur Technik* 76 (2004): 1828–1832, https://doi.org/10.1002/cite.200400087.

5. W. E. Billups, W. E. Walker, and T. C. Shields, "The Palladium-catalysed Carbonylation–dimerization of Butadiene," *Journal of the Chemical Society [Section] D* 0 (1971): 1067, https://doi.org/10.1039/C29710001067.

6. J. Tsuji and M. Takahashi, "Palladium-catalyzed Telomerization of Butadiene With Ammonia," *Journal of Molecular Catalysis* 10 (1980): 107–114, https://doi.org/10.1016/0304-5102(80)80054-x.

7. R. Palkovits, I. Nieddu, R. J. M. K. Gebbink, and B. M. Weckhuysen, "Highly Active Catalysts for the Telomerization of Crude Glycerol With 1,3-butadiene," *Chemsuschem* 1 (2008): 193–196, https://doi.org/10.1002/cssc.200700147.

8. R. Palkovits, I. Nieddu, C. A. Kruithof, R. J. M. Klein Gebbink, and B. M. Weckhuysen, "Palladium-Based Telomerization of 1,3-Butadiene With Glycerol Using Methoxy-Functionalized Triphenylphosphine Ligands," *Chemistry—A European Journal* 14 (2008): 8995–9005, https://doi.org/10.1002/chem.200800792.

9. R. Palkovits, A. N. Parvulescu, P. J. C. Hausoul, C. A. Kruithof, R. J. M. Klein Gebbink, and B. M. Weckhuysen, "Telomerization of 1,3-butadiene With Various Alcohols by Pd/TOMPP Catalysts: New Opportunities for Catalytic Biomass Valorization," *Green Chemistry* 11 (2009): 1155, https://doi.org/10.1039/b904274a.

10. P. J. C. Hausoul, A. N. Parvulescu, M. Lutz, et al., "Mechanistic Study of the Pd/TOMPP-Catalyzed Telomerization of 1,3-Butadiene With Biomass-Based Alcohols: On the Reversibility of Phosphine Alkylation," *Chemcatchem* 3 (2011): 845, https://doi.org/10.1002/cctc.201100048.

11. P. J. C. Hausoul, P. C. A. Bruijnincx, B. M. Weckhuysen, and R. J. M. Klein Gebbink, "Pd/TOMPP-catalyzed Telomerization of 1,3-butadiene: From Biomass-based Substrates to New Mechanistic Insights," *Pure and Applied Chemistry* 84 (2012): 1713–1727, https://doi.org/10.1351/PAC-CON-11-12-06.

12. P. J. C. Hausoul, M. Lutz, J. T. B. H. Jastrzebski, P. C. A. Bruijnincx, B. M. Weckhuysen, and R. J. M. Klein Gebbink, "Mechanistic Study of the Pd/TOMPP-Catalyzed Telomerization of 1,3-Butadiene: Influence of

Aromatic Solvents on Bis-Phosphine Complex Formation and Regioselectivity," *Organometallics* 32 (2013): 5047–5057, https://doi.org/10.1021/om400246a.

13. P. J. C. Hausoul, S. D. Tefera, J. Blekxtoon, P. C. A. Bruijnincx, R. J. M. Klein Gebbink, and B. M. Weckhuysen, "Pd/TOMPP-catalysed Telomerisation of 1,3-butadiene With Lignin-type Phenols and Thermal Claisen Rearrangement of Linear Telomers," *Catalysis Science & Technology* 3 (2013): 1215–1223, https://doi.org/10.1039/C2CY20522J.

14. J. Fritsch, F. Drache, G. Nickerl, W. Böhlmann, and S. Kaskel, "Porous Phosphorus-based Element Organic Frameworks: A New Platform for Transition Metal Catalysts Immobilization," *Microporous and Mesoporous Materials* 172 (2013): 167–173, https://doi.org/10.1016/j.micromeso.2012.12.049.

15. P. J. C. Hausoul, T. M. Eggenhuisen, et al., "Development of a 4,4′-biphenyl/Phosphine-based COF for the Heterogeneous Pd-catalysed Telomerisation of 1,3-butadiene," *Catalysis Science & Technology* 3 (2013): 2571, https://doi.org/10.1039/c3cy00188a.

16. M. Ashour and M. Wink, "Jonathan Gershenzon in Annual Plant Reviews" *Biochemistry of Plant Secondary Metabolism* (John Wiley & Sons, Ltd, 2010), pp. 258–303.

17. J. Beger, C. Duschek, and H. Reichel, "VIII. Palladiumkomplexkatalysierte Dimerisierung und Telomerisierung von Methylsubstituierten Butadienen im Alkoholischen Medium," *Journal für Praktische Chemie* 315 (1973): 1077, https://doi.org/10.1002/prac.19733150611.

18. R. Berger and W. Gaube, "Zur Telomerisierung von Isopren mit Palladium-Komplexen bei niedriger Temperatur," *Journal für Praktische Chemie* 327 (1985): 643–648, https://doi.org/10.1002/prac.19853270415.

19. A. Behr, T. Fischer, M. Grote, and D. Schnitzmeier, "Verfahrenskonzepte zur übergangsmetallkatalysierten Telomerisation von Isopren mit Methanol," *Chemie Ingenieur Technik* 74 (2002): 1586–1591, https://doi.org/10.1002/1522-2640(20021115)74:11⟨1586::AID-CITE1586⟩3.0.CO;2-J.

20. W. Gaube and H. Stegemann, "Zur Palladiumkatalysierten Isoprentelomerisierung in Alkoholischen Medien und Deren Folgereaktionen," *Journal für Praktische Chemie* 326 (1984): 729, https://doi.org/10.1002/prac.19843260504.

21. S. M. Maddock and M. G. Finn, "Palladium-Catalyzed Head-to-Head Telomerization of Isoprene With Amines," *Organometallics* 19 (2000): 2684–2689, https://doi.org/10.1021/om000286g.

22. R. Jackstell, A. Grotevendt, D. Michalik, L. El Firdoussi, and M. Beller, "Telomerization and dimerization of isoprene by in situ generated palladium–carbene catalysts," *Journal of Organometallic Chemistry* 692 (2007): 4737–4744, https://doi.org/10.1016/j.jorganchem.2007.06.039.

23. A. A. Beloglazkin, S. A. Rzhevsky, E. A. Drokin, et al., "Study of the Telomerization Reaction of Isoprene With Methanol Catalyzed by N-Heterocyclic Carbene Pd(II) Complexes Using Mass Spectrometry and NMR Spectrometry," *Journal of Analytical Chemistry* 78 (2023): 1879–1890, https://doi.org/10.1134/S1061934823140022.

24. S. A. Rzhevskiy, M. A. Topchiy, V. N. Bogachev, et al., "NHC Pdii Complexes for the Solvent-free Telomerisation of Isoprene With Methanol," *Mendeleev Communications* 31 (2021): 478–480, https://doi.org/10.1016/j.mencom.2021.07.013.

25. M. A. Topchiy, A. A. Ageshina, S. A. Rzhevskiy, L. I. Minaeva, M. S. Nechaev, and A. F. Asachenko, "Solvent-free Telomerization of Isoprene With Alcohols Catalyzed by Palladium(II) Carbene Complexes," *Russian Chemical Bulletin* 71 (2022): 940–945, https://doi.org/10.1007/s11172-022-3494-2.

26. S. K. Kaiser, Z. Chen, D. Faust Akl, S. Mitchell, and J. Pérez-Ramírez, "Single-Atom Catalysts Across the Periodic Table," *Chemical reviews* 120 (2020): 11703–11809, https://doi.org/10.1021/acs.chemrev.0c00576.

27. X.-F. Yang, A. Wang, B. Qiao, J. Li, J. Liu, and T. Zhang, "Single-atom Catalysts: A New Frontier in Heterogeneous Catalysis," *Accounts of chemical research* 46 (2013): 1740–1748, https://doi.org/10.1021/ar300361m.

28. A. Wang, J. Li, and T. Zhang, "Heterogeneous Single-atom Catalysis," *Nature Reviews Chemistry* 2 (2018): 65–81, https://doi.org/10.1038/s41570-018-0010-1.

29. N. Cheng, L. Zhang, K. Doyle-Davis, and X. Sun, "Single-Atom Catalysts: From Design to Application," *Electrochemical Energy Reviews* 2 (2019): 539–573, https://doi.org/10.1007/s41918-019-00050-6.

30. Q. Wang and D. Astruc, "State of the Art and Prospects in Metal–Organic Framework (MOF)-Based and MOF-Derived Nanocatalysis," *Chemical reviews* 120 (2020): 1438–1511, https://doi.org/10.1021/acs.chemrev.9b00223.

31. X. Feng, X. Ding, and D. Jiang, "Covalent Organic Frameworks," *Chemical Society reviews* 41 (2012): 6010, https://doi.org/10.1039/c2cs35157a.

32. K. Geng, T. He, R. Liu, et al., "Covalent Organic Frameworks: Design, Synthesis, and Functions," *Chemical reviews* 120 (2020): 8814, https://doi.org/10.1021/acs.chemrev.9b00550.

33. P. Kaur, J. T. Hupp, and S. T. Nguyen, "Porous Organic Polymers in Catalysis: Opportunities and Challenges," *ACS Catalysis* 1 (2011): 819–835, https://doi.org/10.1021/cs200131g.

34. F. Benvenuti, C. Carlini, A. M. Raspolli Galletti, G. Sbrana, M. Marchionna, and R. Patrini, "1,3-butadiene telomerization With methanol catalyzed by heterogenized palladium complexes," *Journal of Molecular Catalysis A: Chemical* 137 (1999): 49–63, https://doi.org/10.1016/S1381-1169(98)00074-0.

35. B. Estrine, R. Soler, C. Damez, S. Bouquillon, F. Hénin, and J. Muzart, "Recycling in telomerization of butadiene With methanol and phenol: Pd–KF/Al 2 O 3 as an active heterogeneous catalyst system," *Green Chemistry* 5 (2003): 686–689, https://doi.org/10.1039/B311129F.

36. A. N. Parvulescu, P. J. C. Hausoul, P. C. A. Bruijnincx, et al., "Telomerization of 1,3-Butadiene With Biomass-Derived Alcohols Over a Heterogeneous Pd/TPPTS Catalyst Based on Layered Double Hydroxides," *ACS Catalysis* 1 (2011): 526–536, https://doi.org/10.1021/cs1001477.

37. Z. Wang, S. Hasegawa, K. Motokura, S. Kuang, and Y. Yang, "A Single-Atom Pd Catalyst Anchored on a Porous Organic Polymer for Highly Efficient Telomerization of 1,3-Butadiene With Methanol," *Industrial & Engineering Chemistry Research* 62 (2023): 3151–3156, https://doi.org/10.1021/acs.iecr.2c04672.

38. X. Zhang and B. Yu, "Boosting the Feasibility of Heterogeneous Telomerization of 1,3-butadiene With Methanol by Low-surface-area N-heterocyclic Carbene-functionalized Hypercrosslinked Polymers," *Chemical Engineering Journal* 484 (2024): 149580, https://doi.org/10.1016/j.cej.2024.149580.

39. L. Torrente-Murciano, D. Nielsen, R. Jackstell, M. Beller, K. Cavell, and A. A. Lapkin, "Selective Telomerisation of Isoprene With Methanol by a Heterogeneous Palladium Resin Catalyst," *Catalysis Science & Technology* 5 (2015): 1206–1212, https://doi.org/10.1039/c4cy01320d.

40. P. J. C. Hausoul and T. M. Eggenhuisen, "Development of a 4,4′-biphenyl/Phosphine-based COF for the Heterogeneous Pd-catalysed Telomerisation of 1,3-butadiene," *Catalysis Science & Technology* 3 (2013): 2571, https://doi.org/10.1039/C3CY00188A.

41. P. J. C. Hausoul, C. Broicher, R. Vegliante, C. Göb, and R. Palkovits, "Solid Molecular Phosphine Catalysts for Formic Acid Decomposition in the Biorefinery," *Angewandte Chemie International Edition* 55 (2016): 5597–5601, https://doi.org/10.1002/anie.201510681.

42. A. Kann, H. Hartmann, A. Besmehn, P. J. C. Hausoul, and R. Palkovits, "Hydrogenation of CO2 to Formate Over Ruthenium Immobilized on Solid Molecular Phosphines," *Chemsuschem* 11 (2018): 1857–1865, https://doi.org/10.1002/cssc.201800413.

43. J. C. Baums, I. Kappel, A. Meise, et al., "Additive-Free, Aqueous CO 2 Hydrogenation With Ru/Polyphosphine-Based Solid Molecular Catalysts," *Chemcatchem* 17 (2025), https://doi.org/10.1002/cctc.202402048.

44. K. P. C. Vollhardt, *Organische Chemie*, ed. N. E. Schore (VCH, 1995).

45. H. Anderson, N. Heldt, and K. Heldt, "Kalorimetrische Optimierung der Telomerisierung von Isopren," *Chemie Ingenieur Technik* 66 (1994): 69, https://doi.org/10.1002/cite.330660110.

46. A. Döhring, P. W. Jolly, R. Mynott, K.-P. Schick, and G. Wilke, "„$\eta$1,$\eta$3-Octadienediyl-palladium Complexes," *Zeitschrift für Naturforschung B* 36 (1981): 1198.

47. P. W. Jolly, "$\eta$ 3 -Allylpalladium Compounds," *Angewandte Chemie International Edition in English* 24 (1985): 283–295, https://doi.org/10.1002/anie.198502831.

48. P. W. Jolly, R. Mynott, B. Raspel, and K. P. Schick, "Intermediates in the palladium-catalyzed reactions of 1,3-dienes. The reaction of (.eta.1,.eta.3-octadiendiyl)palladium complexes With acidic substrates," *Organometallics* 5 (1985): 473–481, https://doi.org/10.1021/om00134a014.

49. R. Benn, P. W. Jolly, R. Mynott, et al., "Intermediates in the Palladium-Catalyzed Reactions of 1,3-Dienes. 2.1 Preparation and Structure of (n1,n3-Octadienediyl)paliadium Complexes," *Organometallics* 4 (1985): 1945.

50. S. Seidel, I. Kappel, C. Weidenthaler, P. J. Hausoul, and R. Palkovits, "Porous BINAP-based Polyaromatic Polymers for the Continuous Base-free Ru-catalysed Decomposition of Aqueous Formic Acid," *Journal of Catalysis* 438 (2024): 115712, https://doi.org/10.1016/j.jcat.2024.115712.

51. M. Vennewald and N. M. Sackers, "Dynamics of Palladium Single-atoms on Graphitic Carbon Nitride During Ethylene Hydrogenation," *Journal of Catalysis* 421 (2023): 134, https://doi.org/10.1016/j.jcat.2023.03.011.

52. K. V. A. Birkelbach and H. Hartmann, "Enabling the Terpyridine Ligand Motif for Ir-based Solid Molecular Catalysts," *EES Catalysis* 3 (2025): 701, https://doi.org/10.1039/D4EY00281D.

53. B. S. Bouley, D. Y. Bae, S. Chakrabarti, M. Rosen, R. D. Kennedy, and L. M. Mirica, "Insights Into the Mechanism of Active Catalyst Generation for the PdII(acac)2/PPh3 System in the Context of Telomerization of 1,3-butadiene," *Chemical Science* 16 (2025): 15486, https://doi.org/10.1039/d5sc02171e.

54. Z. Kanda, Y. Nakamura, and S. Kawaguchi, "The Terminal-Carbon-Bonded Palladium(II) Complexes of Acetylacetone," *Chemistry Letters* 5 (1976): 199–200, https://doi.org/10.1246/cl.1976.199.

55. D. S. Suslov, M. V. Bykov, Z. D. Abramov, et al., "Cationic palladium(II)–acetylacetonate complexes containing phosphine and aminophosphine ligands and their catalytic activities in telomerization of 1,3-butadiene With methanol," *Journal of Organometallic Chemistry* 923 (2020): 121413, https://doi.org/10.1016/j.jorganchem.2020.121413.

## Supporting Information

Additional supporting information can be found online in the Supporting Information section.

The supporting information contains synthesis procedures, characterization of the polymers including NMR-MAS, BET nitrogen physisorption, XRD, TG, SEM, and XAS Data, as well as catalysis procedures.

**Supporting File:** cctc70732-sup-0001-SuppMat.docx.